ACS APPLIED MATERIALS & INTERFACES

Research Article

www.acsami.org

Molecular Layer Deposition of an Organic-Based Magnetic Semiconducting Laminate

Chi-Yueh Kao,[†] Jung-Woo Yoo,[‡] Yong Min,[‡] and Arthur J. Epstein*[,†,‡]

[†]Department of Chemistry, The Ohio State University, Columbus, Ohio 43210-1173, United States

[‡]Department of Physics, The Ohio State University, Columbus, Ohio 43210-1117, United States

Supporting Information

ABSTRACT: Organic-based magnets are intriguing materials with unique magnetic and electronic properties that can be tailored by chemical methodology. By using molecular layer deposition (MLD), we demonstrate the thin film fabrication of V[TCNE: tetracyanoethylene]$_x$, of the first known room temperature organic-based magnet. The resulting films exhibit improvement in surface morphology, larger coercivity (80 Oe), and higher Curie temperature/thermal stability (up to 400 K). Recently, the MLD method has been widely studied to implement fine control of organic film growth for various applications. This work broadens its application to magnetic and charge transfer materials and opens new opportunities for metal−organic hybrid material development and their applications in various multilayer film device structures. Finally, we demonstrate the applicability of the multilayer V[TCNE]$_x$ as a spin injector combining LSMO, an standard inorganic magnetic semiconductor, for spintronics applications.

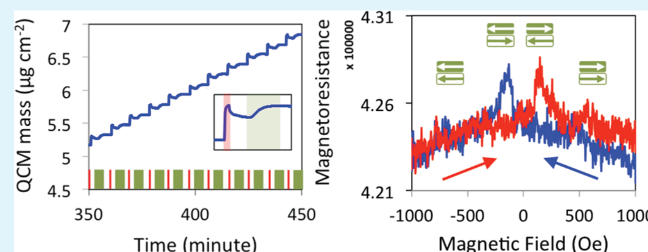

KEYWORDS: *organic-based magnet, molecular layer deposition, magnetic semiconductor, organic spintronics, V[TCNE]$_x$*

1. INTRODUCTION

Organic/molecular-based magnets have been studied since the 1980s. Since then, many intriguing magnetic and optical properties have been discovered.[1−5] The research on the materials has been targeted for the memory applications, as some of the materials have shown unique magnetic bistabilities and light-tunabilities therein.[6,7] The recent incorporation of this type of materials for the spintronic device suggests potential new application of these materials.[8] In particular, the coexistence of room temperature magnetic ordering and semiconductor properties in compounds such as V[TCNE]$_x$,[5,9] should introduce intriguing opportunities for future hybrid electronics.[8,10] Organic materials have been important alternatives to inorganic materials and have shown significant impact on devices such as light-emitting diodes and transistors. Organic/molecular-based magnetic materials could be promising candidates for the future organic/molecular electronic, magnetic, and spintronic applications.

To incorporate the organic-based magnet as a building block for device fabrication, the precise control of the film growth has to be made. So far, several methods have been employed to fabricate thin film V[TCNE]$_x$.[11−13] Among these methods, chemical vapor deposition (CVD) with precursors $V(CO)_6$ and TCNE as precursors has been the most widely studied technique.[11] This approach produces a structure that is homogeneous in stoichiometry with variation in thickness, which introduces challenge for the integration of these magnetic films into multilayer devices.[14] Therefore, a deposition method with better control is needed for further development of these materials and their applications. To achieve a thin V[TCNE]$_x$ film, a physical vapor deposition (PVD)-based method under ultra high vacuum (UHV) has been used to deposit thin films with the thickness of only few tens of nanometers.[13] However, thin films made by this method have shown undesired bonding, such as the bonding between metal atom and C−C double bond in TCNE molecule, which may affect the film properties.[15] Therefore, developing molecular level control of film growth of V[TCNE]$_x$ is of great interest and will inspire various electronic and spintronic applications of the organic/molecular-based magnetic materials.

MLD is an analogue to atomic layer deposition (ALD) which is a technique to grow thin films by exposing the substrates to different precursors alternatively and sequentially.[16,17] The self-limiting nature of the MLD process allows the thickness of the film to be controlled within a monolayer as well as results in highly conformal films. In addition, ALD prepared film has shown superior performance on growing uniform film on structure with high aspect ratio.[18] Until now, the studies of MLD have covered several types of materials, such as organic polymers,[19−23] organic−inorganic hybrid materials,[24,25] small molecules,[26] self-assembled monolayer derivatives,[27,28] and molecular heterolayers.[19] Potential applications of these materials are of wide variety, such as dielectric layer, semiconducting layer, sacrificial layer, growth template, etc.,

Received: August 29, 2011
Accepted: December 15, 2011
Published: January 4, 2012

 © 2012 American Chemical Society

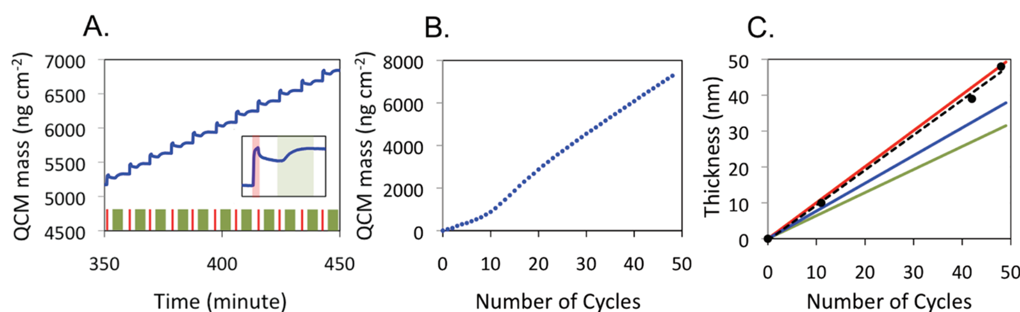

Figure 1. Growth behavior monitored by QCM. (A) QCM response of several cycles of MLD of V[TCNE]$_x$. The red and green bars indicate the exposure of $V(CO)_6$ and TCNE respectively. The inset shows a magnified graph of mass change within one cycle. (B) QCM mass vs number of MLD cycle. (C) Thickness vs number of cycle measured by AFM. Black dots represent data points that taken from thin films with different MLD cycles. The black dashed line is the trend line which has a slope of 0.98. Solid lines are theoretical values of different binding orientation based on calculated V-TCNE-V distances.[29] The red line represents a binding fashion of trans-orientation. The blue and green lines represent two types of cis-orientations.

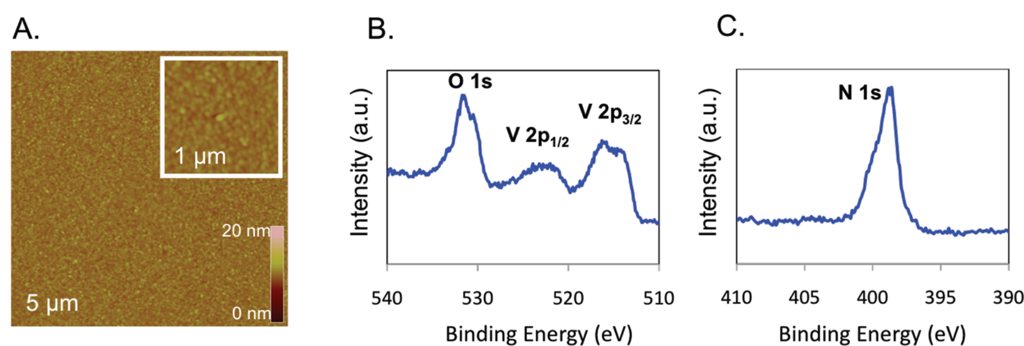

Figure 2. (A) AFM images of thin film of 42 cycles with image dimension of 5 μm × 5 and 1 μm × 1 μm (inset). The scale bar represents heighth from 0 to 20 nm. (B) XPS spectrum of V 2p and O 1s where the bands located ~515 and ~523 eV are from V 2p 3/2 and V 2p 1/2 respectively, and the band at ~532 eV is from O 1s. (C) XPS spectrum of N 1s.

which suggests MLD a promising technique for fabricating organic-based thin films for practical applications. In this report, an example of MLD to fabricate a magnetic material is demonstrated.

2. EXPERIMENTAL SECTION

Precursor Preparation. Tetracyanoethylene (TCNE) and vanadium hexacarbonyl ($V(CO)_6$) were used as precursors in this work. TCNE was purchased from Sigma-Aldrich and purified by sublimation with activated carbon before use. $V(CO)_6$ was synthesized according to the literature. Before and after deposition, both precursors were stored in airtight containers in inert environment in a refrigerator (at −35 °C).

V[TCNE]$_x$ Deposition. The chamber was pumped down with a turbo pump system overnight before performing deposition. The base pressure was <1 × 10^{-5} Torr. The chamber and precursors were at room temperature during the entire deposition process. The typical MLD sequence for one cycle was: (i) $V(CO)_6$ exposure: chamber sealed for ~50 s, a pulse of $V(CO)_6$ was introduced to the chamber for the first 2 s in this step; (ii) evacuation: ~100 s; (iii) TCNE exposure: samples were exposed to TCNE for ~300 s while the chamber continued evacuating; (iv) evacuation: ~150 s. The pressures were about 1 × 10^{-1} Torr during step i and 1 × 10^{-4} Torr during step iii. Upon the completion of the deposition, the chamber including the samples was then transferred into an Ar-filled glovebox for further process/analysis.

QCM Measurement. The quartz crystal microbalance (QCM) was connected to a XTM/2 (Inficon) monitor. The data was recorded by a PC. The mass gain was calibrated by polished 6 MHz quartz crystal discs (Inficon). Crystals were deposited with 20 nm of SiO_x by e-beam deposition prior to MLD.

Sample Analysis. All samples for analysis were deposited on double-side polished Si(111) substrates with an exception of the air-stability measurement that was deposited on a glass substrate. Atomic force microscopy (AFM) images were taken using a Dimension 300 SPM by Digital Instruments. X-ray photoelectron spectra (XPS) were taken from thin film deposited on Si substrate and measured by a Kratos Axis Ultra XPS. Samples for XPS were transferred to the chamber of the spectrometer with an airtight transfer tool to reduce air exposure. Transmission infrared (IR) spectrum was taken from a Perkin-Elmer Spectrum 100 FT-IR spectrometer. Samples for IR measurement were sealed in an airtight cell during measurement. Magnetic properties and temperature-dependent electrical properties were measured from a superconducting quantum interference device (SQUID) magnetometer and a physical properties measurement system (MPMS and PPMS by Quantum Design) respectively. Samples for thin film air-stability were deposited on a glass substrate with Al electrodes, and the resistance was measured with a Keithley 617 electrometer.

3. RESULTS AND DISCUSSION

The MLD was performed in a homemade close-type system where no carrier gas was introduced. The base pressure of the system was ~1 × 10^{-5} Torr, and the deposition process was done at room temperature. During the MLD process, substrates were exposed to $V(CO)_6$ and TCNE alternatively, and each exposure step was followed by an evacuation step. One set of exposure and evacuation steps for both precursors is defined as one cycle here. The ideal surface reactions are

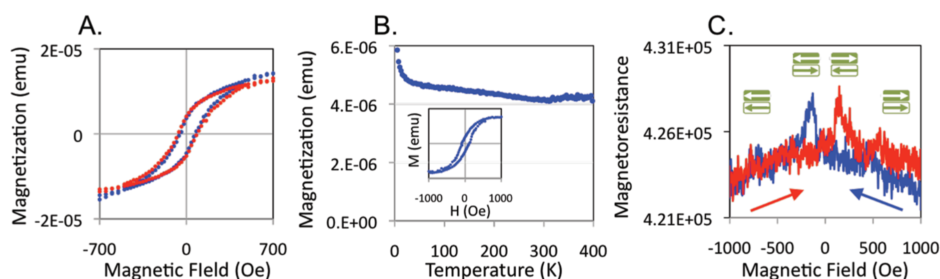

Figure 3. Magnetic properties and magnetoresistance. (A) Magnetization versus magnetic field was measured for a sample of 48 MLD cycles. The sample was measured at 5 K (blue dots) and 300 K (red dots). The film was deposited on a Si substrate then covered by 20 nm of aluminum as a barrier to oxidation. (B) Temperature dependence of magnetization under magnetic field of 200 Oe, while the inset shows the hysteresis loop measured at 400 K. (C) The magnetoresistance curves of a V(TCNE)$_x$(50 nm)/LAO(1.2 nm)/LSMO(50 nm) junction measured at 20 K with a bias field of 1.5 V. The red (blue) dots are the data collected with increasing (decreasing) magnetic field.

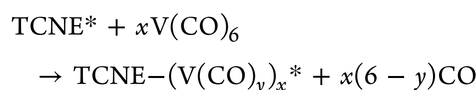

$$\mathrm{TCNE}^* + x\mathrm{V(CO)}_6 \rightarrow \mathrm{TCNE{-}(V(CO)}_y)_x{}^* + x(6-y)\mathrm{CO}$$

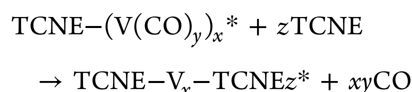

$$\mathrm{TCNE{-}(V(CO)}_y)_x{}^* + z\mathrm{TCNE} \rightarrow \mathrm{TCNE{-}V}_x\mathrm{{-}TCNE}z^* + xy\mathrm{CO}$$

where the asterisks indicate the surface species.

To investigate the behavior of MLD, the deposition was monitored by a quartz crystal microbalance (QCM). Figure 1a shows the response of QCM to deposited mass during several cycles as it reached steady growth state. The deposited mass increased upon the exposure to $V(CO)_6$ and TCNE vapor. The inset in Figure 1a shows the response of QCM within one cycle, which demonstrates the self-limiting feature of MLD. Comparing to $V(CO)_6$, the exposure of TCNE results in a lower absorption rate. The low rate is attributed to the low vapor pressure of TCNE which is about 3 orders of magnitude lower than that of $V(CO)_6$. Figure 1b shows mass gain versus number of cycle for a deposition of 48 cycles. The deposition holds an overall constant growth rate with a curvature in first 15 cycles, whereas the curvature is a sign of the initial nucleation process.

This MLD deposition results in an average growth rate measured by AFM of ~0.98 nm per cycle (Figure 1c). This value is in reasonable range where, corresponds to the distances of two vanadium atoms in V-TCNE-V structures of cis- and trans-orientations.[29] Incorporating the result from QCM, density of the film can be estimated as ~1.5 g/cm^3 from the mass gain per cycle (~150 ng/cm^2), which is larger than that of solution-made V[TCNE]$_{\sim 2}$ that is approximately 1 g/cm^3.[30] The appearance of the film was visually uniform with no sign of uneven thickness. Figure 2a shows an AFM image of a MLD deposited film displaying uniform surface morphology over the whole scan area with spherical surface feature. The surface root-mean-square roughness was measured to be ~0.5 nm, which is a typical roughness for ALD/MLD processed films.

X-ray photoelectron spectroscopy (XPS) was used to determine to the chemical composition of the film. The elemental analysis of a sample shows that the thin film has a chemical composition of $VC_{5.3}N_{2.5}O_{1.3}$, which suggests a TCNE to V ratio of 0.63. Without considering the adventitious carbon that is normally located at 284.8 eV, the C to N ratio is 1.58:1 that is close to that of TCNE. The oxygen content can be mainly attributed to surface oxidation during as well as after deposition. The presence of oxygen inside the film is further evident by XPS analysis after removing surface oxide by in situ argon sputtering, that reveals a ratio close or lower than 0.6 O per V atom in the bulk of the film (see the Supporting Information).

In Figure 2a, the XPS showed two V 2p bands that range from 528 to 510 eV are due to spin−orbit splitting. In each band, the features that centered at 513.8 and 521.5 eV are attributed to V^{2+}, whereas the high binding energy parts are assigned to oxide species.[11] The corresponding oxygen band for oxides was located at ~531 eV. In Figure 2b, a broad band of N 1s was observed with a weak shakeup satellite on the high binding energy side. The shape of the band is similar to that for N of V[TCNE]$_x$ films made from CVD and PVD.[11,13] The band can be tentatively attributed to [TCNE]$^-$ and [TCNE]$^{2-}$ which was evident by FTIR spectroscopy (see the Supporting Information). Although the overall spectra are consistent with V[TCNE]$_{\sim 2}$ films made by CVD and PVD, the contents of the oxidized species are higher in MLD sample which may due to oxidation during deposition.

Magnetic properties of the MLD-made film were measured by a SQUID magnetometer. The hysteresis loops of M vs H are shown in Figure 3a demonstrates that this film is a room-temperature magnet with coercivity of ~80 Oe at both 5 and 300 K. It should be noted that coercive fields of the films vary slightly from batch to batch. The temperature dependence of magnetization is shown in Figure 3b. The curve shows no significant drop as temperature rises up to 400 K, the highest temperature accessible in the SQUID magnetometer which suggests that the MLD-made film has a higher Curie temperature (T_c) and/or thermal stability as compared to CVD-made film. The hysteresis loop can clearly be seen even at 400 K (inset in Figure 3b). A local maximum in M vs H can be observed at temperature above 300 K. The origin of this maximum is not yet fully understood, though it may indicate the presence of glass or cluster glass behavior resulting from incomplete structural order that needs further study to elucidate. In addition to magnetic properties, the activation energy of charge transport has been measured as ~0.45 eV, which is lower than that of CVD film (0.5 eV)[9] (see the Supporting Information). The air stability in terms of film electrical resistance has been measured (see Supporting Information). Once the thin film is exposed to air, the film resistance increased 50% within the first day and then starts leveling off with an increase of only 13% in the following 4 days. The subtle continuous increase of film resistance is in part due to the applied voltage. Base on the film resistance result,

the MLD-made film shows much improved air stability as compared to CVD-made film.

The feasibility of MLD laminated $V(TCNE)_x$ films for use as the spin polarizing layer in devices was tested via the standard magnetic tunnel junction structure. 50 nm of $La_{2/3}Sr_{1/3}MnO_3$ (LSMO) film on (001) $(LaAlO_3)_{0.3}(Sr_2AlTaO_6)_{0.7}$ substrate was employed for the counter magnetic layer and a layer of three unit cells of $LaAlO_3$ (LAO) was used for the insulating barrier. The size of devices was 200 μm × 200 μm. Both LSMO and LAO thin films were prepared via pulsed laser deposition.[8] Figure 3c shows magnetoresistance curves for an in-plane magnetic field in a hybrid magnetic junction of MLD deposited $V(TCNE)_x$ (50 nm)/LAO(1.2 nm)/LSMO(80 nm) at 20 K with an applied bias of 1.5 V. The red lines represent the data recorded during a positive sweep of the magnetic field. The blue line represent the data collected during negative field sweeping. With sweeping of the magnetic field, the device resistance becomes higher when the magnetizations of two magnetic layers become antiparallel. The magnetoresistance curves clearly show spin polarizing nature of MLD laminated $V(TCNE)_x$ film. The small percentage of magnetoresistance in this hybrid magnetic tunnel junction may be attributed to the initial growth of MLD $V(TCNE)_x$ film. The growth of MLD film starts to nucleate on the substrate surface and needs around 10−15 deposition cycles before it starts to cover the whole area at each cycle (see Figure 1b). This initial growth mechanism could lower the spin polarization of the MLD film near the interface, where it affects the injected electron spin polarization at the device interface. Following several approaches can be made to improve this hybrid magnetic tunnel junction. (i) Selecting materials or engineering the surface by methods such as applying self-assembled monolayer that help initial growth of MLD-made $V[TCNE]_x$ film and improve interfacial spin polarization. (ii) Precise control of optimal condition for MLD deposition could also help to improve interface quality. (iii) Scaling down the size of device will reduce the effect of defects at the interface.

4. CONCLUSION

In summary, thin films of the laminate of vanadium and TCNE were successfully fabricated via MLD. The resulting film is uniform with film thickness as low as few tens of nanometers. It shows a large coercive field and high T_c and/or thermal-stability. Air-stability is significantly improved as well. It has been tested as active layer in a standard magnetic junction structure, and the magnetoresistance has been observed. Meanwhile, room-temperature MLD of charge transfer/magnetic thin film was demonstrated for the first time. With the magnetic and electronic properties and the simplicity of the fabrication method, thin film organic-based magnets are promising materials for development of next-generation spin-related applications.

■ ASSOCIATED CONTENT

Ⓢ Supporting Information

Percent concentration change of V and O upon in situ Ar sputtering, FTIR, measurement of activation energy, and measurement of air stability. This material is available free of charge via the Internet at http://pubs.acs.org.

■ AUTHOR INFORMATION

Corresponding Author

*Phone: (614)292-1133. Fax: (614)292-3706. E-mail: epstein@mps.ohio-state.edu.

■ ACKNOWLEDGMENTS

This work was supported in part by AFOSR Grant FA9550-06-1-0175, DOE Grant DE-FG02-01ER45931, NSF Grant DMR-0805220, and Center for Emergent Materials at the Ohio State University, an NSF MRSEC Grant DMR-0820414.

■ REFERENCES

(1) Miller, J. S.; Calabrese, J. C.; Epstein, A. J.; Bigelow, R. W.; Zhang, J. H.; Reiff, W. M. *J. Chem. Soc., Chem. Commun.* **1986**, 1026.
(2) Chittipeddi, S.; Cromack, K. R.; Miller, J. S.; Epstein, A. J. *Phys. Rev. Lett.* **1987**, *58*, 2695.
(3) Kahn, O. *Angew. Chem., Int Ed.* **1985**, *24*, 834.
(4) Awaga, K.; Sugano, T.; Kinoshita, M. *J. Chem. Phys.* **1986**, *85*, 2211.
(5) Manriquez, J. M.; Yee, G. T.; Mclean, R. S.; Epstein, A. J.; Miller, J. S. *Science* **1991**, *252*, 1415.
(6) Sessoli, R.; Gatteschi, D.; Caneschi, A.; Novak, M. A. *Nature* **1993**, *365*, 141.
(7) Sato, O.; Iyoda, T.; Fujishima, A.; Hashimoto, K. *Science* **1996**, *272*, 704.
(8) Yoo, J. W.; Chen, C. Y.; Jang, H. W.; Bark, C. W.; Prigodin, V. N.; Eom, C. B.; Epstein, A. J. *Nat. Mater.* **2010**, *9*, 638.
(9) Prigodin, V. N.; Raju, N. P.; Pokhodnya, K. I.; Miller, J. S.; Epstein, A. J. *Adv. Mater.* **2002**, *14*, 1230.
(10) Fang, L.; Bozdag, K. D.; Chen, C. Y.; Truitt, P. A.; Epstein, A. J.; Johnston-Halperin, E. *Phys. Rev. Lett.* **2011**, *106*, 156602.
(11) Pokhodnya, K. I.; Epstein, A. J.; Miller, J. S. *Adv. Mater.* **2000**, *12*, 410.
(12) de Caro, D.; Basso-Bert, M.; Sakah, J.; Casellas, H.; Legros, J. P.; Valade, L.; Cassoux, P. *Chem. Mater.* **2000**, *12*, 587.
(13) Carlegrim, E.; Kanciurzewska, A.; Nordblad, P.; Fahlman, M. *Appl. Phys. Lett.* **2008**, *92*, 163308.
(14) Pokhodnya, K. I.; Bonner, M.; Miller, J. S. *Chem. Mater.* **2004**, *16*, 5114.
(15) Carlegrim, E.; Zhan, Y.; Li, F.; Liu, X.; Fahlman, M. *Org. Electron.* **2010**, *11*, 1020.
(16) George, S. M.; Yoon, B.; Dameron, A. A. *Acc. Chem. Res.* **2009**, *42*, 498.
(17) George, S. M. *Chem Rev* **2010**, *110*, 111.
(18) Graugnard, E.; Roche, O. M.; Dunham, S. N.; King, J. S.; Sharp, D. N.; Denning, R. G.; Turberfield, A. J.; Summers, C. J. *Appl. Phys. Lett.* **2009**, *94*, 263109.
(19) Loscutoff, P. W.; Zhou, H.; Clendenning, S. B.; Bent, S. F. *ACS Nano* **2010**, *4*, 331.
(20) Yoshimura, T.; Tatsuura, S.; Sotoyama, W. *Appl. Phys. Lett.* **1991**, *59*, 482.
(21) Kubono, A.; Yuasa, N.; Shao, H. L.; Umemoto, S.; Okui, N. *Thin Solid Films* **1996**, *289*, 107.
(22) Bitzer, T.; Richardson, N. V. *Appl. Phys. Lett.* **1997**, *71*, 662.
(23) Lee, J. S.; Lee, Y. J.; Tae, E. L.; Park, Y. S.; Yoon, K. B. *Science* **2003**, *301*, 818.
(24) Dameron, A. A.; Seghete, D.; Burton, B. B.; Davidson, S. D.; Cavanagh, A. S.; Bertrand, J. A.; George, S. M. *Chem. Mater.* **2008**, *20*, 3315.
(25) Peng, Q.; Gong, B.; VanGundy, R. M.; Parsons, G. N. *Chem. Mater.* **2009**, *21*, 820.
(26) Nilsen, O.; Klepper, K. B.; Nielsen, H. O.; Fjellvag, H. *ECS Trans.* **2008**, *16*, 3.
(27) Lee, B. H.; Ryu, M. K.; Choi, S. Y.; Lee, K. H.; Im, S.; Sung, M. M. *J. Am. Chem. Soc.* **2007**, *129*, 16034.
(28) Li, Y. H.; Wang, D.; Buriak, J. M. *Langmuir* **2010**, *26*, 1232.
(29) Miller, J. S. *Polyhedron* **2009**, *28*, 1596.

(30) Epstein, A. J.; Miller, J. S. *Francqui Scientific Library* **1999**, *4*, 20.